Proceedings of IMECE2006
2006 ASME International Mechanical Conference Engineering Congress and Exposition
November 5-10, 2006, Chicago, IL, USA

IMECE2006-15046

MODELING BOUNDARY CONDITIONS AND THERMOCOUPLE RESPONSE IN A THERMAL EXPERIMENT*

Vicente J. Romero†
Model Validation and Uncertainty Quantification Dept. 1533
Sandia National Laboratories‡

Joe W. Shelton
Modeling and Simulation Dept. 2991
Sandia National Laboratories

Martin P. Sherman
Model Validation and Uncertainty Quantification Dept. 1533
Sandia National Laboratories

ABSTRACT

A series of experiments have been conducted in an effort to support the experimental characterization of thermally decomposing foam. The hardware consists of a stainless steel cylinder (slug) embedded in a removable epoxy foam (REF). The slug/foam assembly is pressed into a 20-mil thick 3.5-inch diameter by 3.5-inch tall stainless steel can. In the particular experiment considered in this paper, the can was heated from the top by a bank of quartz heating lamps. In modeling the experiment, several non-trivial difficulties were encountered associated with characterization and modeling of the experimental heating conditions. In the paper we share some thought processes and describe the iterative modeling approach required to model the experiment. Novel features of the effort include modeling of embedded thermocouples in our finite-element model of the test unit, and inverse analysis to solve for the magnitude of incident heat flux from the quartz lamps.

INTRODUCTION

A series of experiments have been conducted[1] in an effort to support the experimental characterization of thermally decomposing foam at Sandia National Laboratories. These experiments are conducted with the test hardware depicted in Figure 1. The hardware consists of a stainless steel cylinder ("slug") embedded in a removable epoxy foam (REF). The slug/foam assembly is pressed into a 20-mil thick 3.5-inch diameter by 3.5-inch tall stainless steel can. Hence, the name foam in a can (FIC) will be used to refer to this experiment in the remainder of this document. In the particular experiment considered in this paper, the can was heated from the top (through a hole cutout in the insulation board) by a bank of quartz heating lamps (tubes) shown at the top of the left picture in Figure 1.

The three stainless steel legs holding the FIC unit in place are sharpened at their tips so that contact with the FIC unit is minimized. We assume that negligible conductive heat transfer occurs through these contact points.

The FIC experiments are designed to aid in the development and validation of various foam pyrolytic decomposition and thermal transport models under development at Sandia National Laboratories. These experiments provide excellent data for foam behavioral model development and assessment. However, the focus of this paper is to document the processes and inductive reasoning required to accurately model thermal boundary conditions (BCs), assess the influence that TCs have on local temperature response, and quantify the errors associated with TC measurement and installation effects. In this regard, Figure 2 shows one variant of a finite-element model (FEM) developed to simulate heat transport to, from, and through the FIC unit in the experiments.

THERMOCOUPLE CONSIDERATIONS

All of the TCs in the FIC experiments are ungrounded K-type with 23 mil diameter Inconel sheaths. The TCs located in the 0.375-inch-thick stainless-steel top and bottom plates are inserted into radially drilled holes as shown in Figure 3. Relatively small bias errors (<1% of reading[2,3]) can normally

---

* This paper is declared a work of the U.S. Government and is not subject to copyright protection in the United States. Approved for public release; distribution is unlimited.

† Corresponding author, vjromer@sandia.gov

‡ Sandia is a multiprogram laboratory operated by Sandia Corporation, a Lockheed Martin Company, for the U.S. Department of Energy's National Nuclear Security Administration under Contract DE-AC04-94AL85000.

Figure1. FIC test hardware and experimental setup

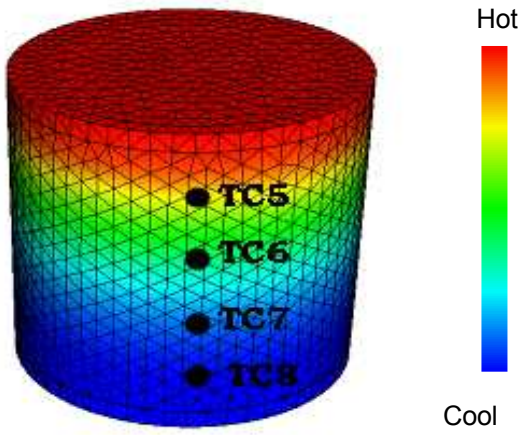

Figure 2. Finite-element model of heated FIC can with some critical can sidewall thermocouple locations shown (preliminary coarse tetrahedral mesh #1 shown)

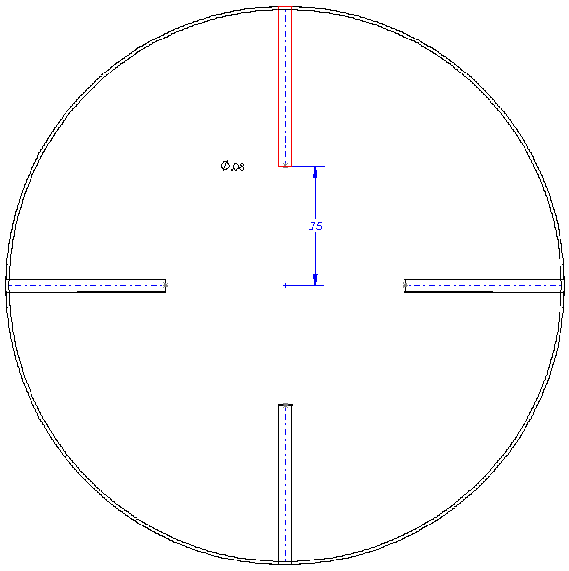

Figure 3. Holes for embedded thermocouples inserted into top and bottom plates of FIC unit.

be expected with such "embedded" or inserted TC leads predominantly parallel to local isotherms. However, the large temperature difference between the heated top plate or "lid" and the ambient temperature, which the TC sheath is exposed to as it exits the drilled hole, may result in a more substantial temperature difference between the TC tip and the bottom of the drilled hole. Therefore, TC behavior is explicitly modeled in the heated plate as described in the next section. Much lower temperatures exist at the bottom plate, so these TCs are not explicitly modeled but associated errors are assumed to be <1% of reading.[2,3] A process for bias correcting the TC data with associated uncertainty in the correction carried along is described in Reference 4.

The TCs on the can wall are strapped to the exterior surface with tack-welded Nichrome strips (see right picture of Figure 1) such that the TC leads are predominantly parallel to the local isotherms set up by heat flow down the can walls. This type of TC installation is expected to yield less than 2% bias error.[5,6] Including these TCs in our FEM would be difficult and computationally expensive (see, e.g., Reference 7. Therefore we have not explicitly modeled them here.

The slug TCs are inserted into drilled holes predominantly perpendicular to the local isotherms. This type of installation results in a more significant error than if the leads lie parallel with the local isotherms. Because the slug TCs are considered critical to evaluation of the various foam thermal transport models, they are explicitly included in the FEM as described in the next section.

All TC leads conduct some heat from their surface locations, thereby perturbing the local temperature of the surface being measured. This effect is accounted for in the simulations only for the slug and heated lid TCs that are explicitly modeled in our FEM. Temperature perturbation effects are not currently included for the TCs on the base and side-walls of the can because these TCs are not explicitly modeled. However, these effects are thought to be insignificant to our analysis.

Other TC reading biases and uncertainties contributed by individual thermocouple-to-thermocouple variations, connector-block effects, and data acquisition system effects are described in References 8 and 9. These sources of error are typically much smaller than those due to installation and temperature perturbation effects. Nevertheless, proper accounting of all the various error sources is at least pedagogically important.

THERMOCOUPLE MODELING IN THE FINITE-ELEMENT MODEL

To provide a FEM of the FIC test unit that can simulate the embedded TCs, a material volume surrounding the TCs is introduced into the model. This volume, which will be referred to as the "Air-Gap" volume, is shown in Figure 4. Partial contact between the TC and the installation hole exists with some effective conductivity between the extremes of perfect contact everywhere and no intimate contact anywhere. These conductivity possibilities are modeled by an uncertain thermal conductivity in the air-gap material bounded between the extremes of stainless steel (the slug and heated lid material) conductivity, and a conductivity equivalent to combined 1-D radial conduction and radiation across the air gap.

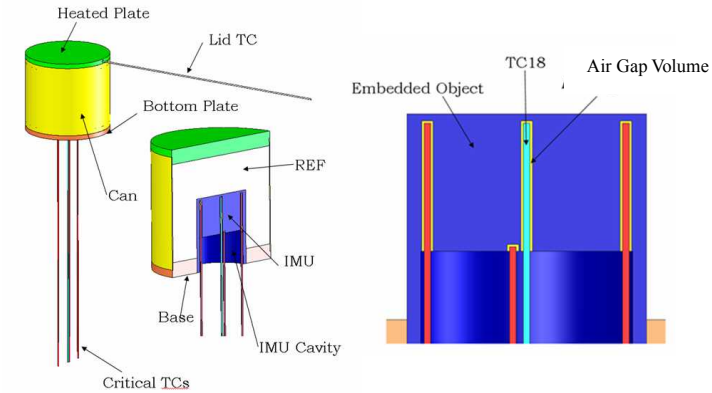

Figure 4. FIC solid model with right picture showing close-up of modeled TCs inserted into drilled holes in slug object. Note yellow Air-Gap volume clearance between inserted TC sheaths and walls of insertion holes.

The Inconel sheath of the TCs is only 0.005 inch thick and is therefore modeled with quadrilateral shell-type finite elements. The insulated core of the TC leads is captured with solid hexahedral elements. To capture the FIC geometry and thermocouples using a reasonable number of finite elements, some minor modifications were required. The outside diameters of the TCs were increased from 0.032 to 0.046 inches. This increase in diameter allows the TC geometry to be captured with slightly larger finite elements. Because of element size constraints propagated to the rest of the 3D model, the use of slightly larger TC elements reduces the number of elements required in the FIC model from order 10^6 elements to order 10^5. The TC installation holes were increased from 0.030 to 0.084 inches. These holes were increased just enough to allow for the meshing of the air-gap volume with a reasonable quality mesh. The sheath conductivity, emissivity, and exposed surface convection coefficient are scaled appropriately to compensate for the artificially large sheath diameter in the model, as detailed in Reference 10.

The exposed portions of the TC sheaths lose heat to the environment by radiation and convection. Specific material properties and heat transfer coefficients (htc) will be presented later. An adiabatic BC is used at the end of the TC leads. This BC is appropriate if the modeled lead is long enough that it's calculated surface temperature reaches the ambient convective/radiative environmental temperature somewhere before the end of the lead. A simulation with nominal values of the convective and radiative parameter uncertainties indicates that the TC leads reached the equilibrium environmental temperature at a location about 2 inches from the exit of the TC holes. Since the TC leads are all 10 inches long in the model, the adiabatic end-BC applied here is appropriate.

EMBEDDED TCS BIAS-ERROR STUDY

To bound the temperature measurement error associated with installation of the TCs, two simulations are performed. The material properties of the air gap volume are varied between a no-contact air case and a perfect-contact SS304 case. For the no-contact case the thermal properties of the air-gap material are temperature-dependent specific heat and density of standard air from Reference 11, and effective conductivity is given by combined 1-D temperature-dependent air conduction and linearized thermal radiation across the gap (see Reference 12).

Figure 5 shows, for the extreme cases of stainless steel (SS) and air fillers in the air-gap volume, the local temperature perturbation due to the presence of the thermocouple: = {temperature of the bottom of the slug central TC installation hole (TC18) in the FEM with the TC leads modeled} minus {temperature in the FEM without the TC in the model}. The addition of the TCs to the FEM show a very small impact on the local temperature of the slug. In the most extreme case of perfect thermal contact between the TC leads (sheath) and the installation hole (as modeled by the stainless steel filler of the air-gap volume), the local temperature depression grows during the transient thermal response of the slug to a maximum value of less than 2.3K by the end of the experiment. Figure 7 shows analogous temperature perturbations caused by the installed TCs in the heated lid. The local temperature depression in the heated lid reaches a high of about 5K during its fast-transient phase of response, and then quickly settles back to a steady-

state value of about 1K during the temperature plateau of the lid (see Figure 12). The local temperature depression is similar whether air or SS is the filler material, presumably due to the significant radiative contribution to heat transfer across the air gap for the high lid temperatures involved.

Figures 6 and 8 provide insight into the error associated with TC installation. They show, for both SS and air fillers in the air-gap volume, the difference in temperature between the TC tip and the bottom of its installation hole: {temperature of the TC tip} minus {temperature of the bottom of installation hole}. The TC installation bias error is negligible (< 0.5K in magnitude whether in the slug or heated lid) for the extreme case of perfect contact between TC and installation hole. However, when the air-gap volume is filled with air for the other extreme of no metal-to-metal conductive contact, the installation bias error becomes non-negligible. In this case, although the heat flux through the lid is much greater than at the site of TC18 in the slug, TC18 has about the same ~5K maximum bias error presumably because its leads are primarily normal to the local isotherms, whereas the lid TC leads wires are in the plane of the local isotherms.

The local temperature perturbation due to presence of the TCs biases temperature readings in the same direction as the bias due to installation effects, so the two add to give total bias on temperature reading. Let

A = temperature of the TC tip

B = temperature at measurement location without the TC present

C = temperature at measurement location when the TC is present

Then, identically, A = A + (C – C) + (B – B) = B + (C - B) + (A - C), where (C - B) is the local temperature perturbation due to the presence of the TC as discussed above and shown in Figures 5 and 7, and (A - C) is the difference shown in Figures 6 and 8 between the TC bead temperature and the local surface temperature due to TC installation contact resistance.

Note that if the TCs were not explicitly modeled in the FEM, the bias effects (C - B) and (A - C) would not normally be accounted for, or would have to come from crude estimates. For instance, for the slug TC #18, the upper total bias error = (C - B) + (A - C) corresponding to an air filler has a ~4K peak and sustained value. This is about 1.3% of reading at the early peak of ~550 seconds but decreases to well less than 1% later in the test (see Figure 16). However, as a percentage of the slug's top-surface temperature rise during the experiment (which is a measure of particular interest in the project), the maximum error is on the order of 40% at 550 seconds, decreasing rapidly to less than 2% of slug temperature rise by the end of the test. These bias magnitudes and percentages are about 50% smaller for the other limit of uncertainty corresponding to a stainless steel Air-Gap filler. For the lid TC, the upper total bias error corresponding to an air filler has a momentary ~4% peak of reading very early into the transient response of the lid (see Figure 12), and then quickly dies to something insignificant thereafter. The lower estimate of total bias error corresponding to a stainless steel Air-Gap filler has a momentary ~2% peak of reading very early and then quickly dies to insignificance thereafter. Certainly, it is sometimes important to quantify TC bias errors with much more precision (in both magnitude and time behavior) than is allowed by "rule of thumb" type bounding estimates.

FINITE ELEMENT MODEL AND SIMULATIONS

Our FEM was developed for simulating heat transfer through decomposing foam to the embedded slug. The solid model used for the FEM is shown in Figure 4. The "HEX1/RES2" model used for the results reported here contains roughly 81,000 hexahedral elements and a similar number of nodes. It has been verified to give spatially and temporally converged temperature predictions. Further details of the FEM and discretization convergence studies can be found in Reference 13. The thermal code used was Sandia's massively parallel code CALORE[14]. A typical 30 minute transient took about 5 hours of simulation time on 6 450MHz processors of a SUN/Solaris compute server.

To simulate the FIC tests seen in Figure 1, several BCs are required. A BC indicative of the linear array of quartz lamps used to heat the FIC lid (heated plate) is required. BCs are also needed to capture the heat lost from the FIC unit due to convection and radiation losses. For the initial condition in the model, the average temperature reading of all 24 TCs in the FIC experiment is used. The standard deviation of the 24 readings is only 1.25K, with a maximum difference of about 2 K from the average.

For the heated lid, a temperature BC driven by TC measurements in the lid is initially used. As Figure 3 shows, TCs at 90-degree intervals around the heated lid are inserted to a depth of one inch radially inward from the lid edge on a plane ¼ of the lid thickness from its heated surface. These TCs measure essentially the same temperature at a given point in time, with a maximum standard deviation of about 6 K over the duration of the test. In light of the limited experimental data about the lid radial temperature profile, a spatially uniform temperature boundary condition (average of the 4 TC temperatures) on the top of the lid is initially assumed for ease of modeling. This approximation will be re-examined later.

NATURAL CONVECTION TO ENVIRONMENT

The natural convection from the walls of the FIC assembly can be approximated with a vertical plate correlation. Using the empirical correlation found in Reference 15, an average wall convective heat transfer coefficient (htc) of 10.5 W/m^2K is calculated for calm ambient air at a temperature of 300 K and a spatial-temporal average wall temperature of 800 K. The htc calculations associated with heat losses from the base plate and the slug partial cavity (illustrated in Figure 4) due to convection

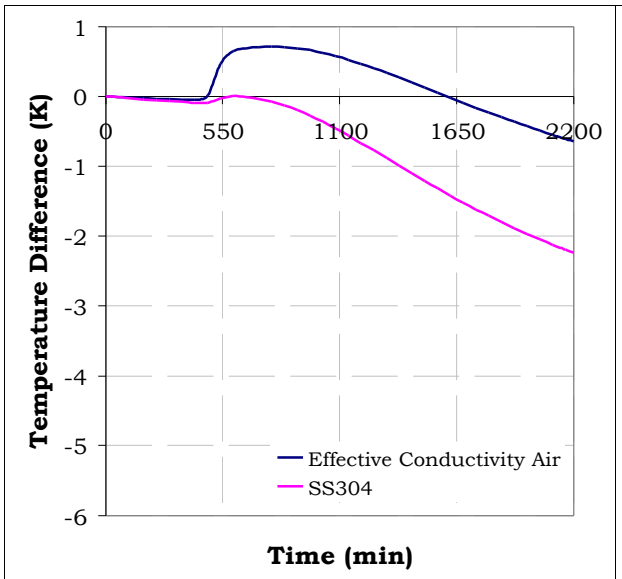

Figure 5. Slug local temperature perturbation due to TC installation

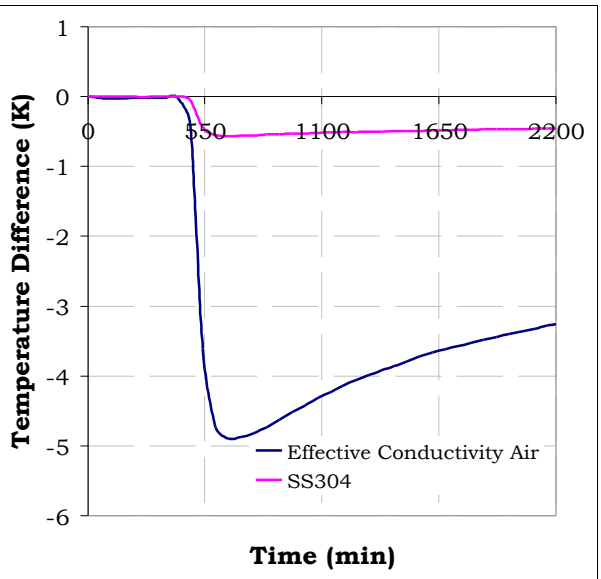

Figure 6. Slug TC temperature indication error (bias) due to installation effects

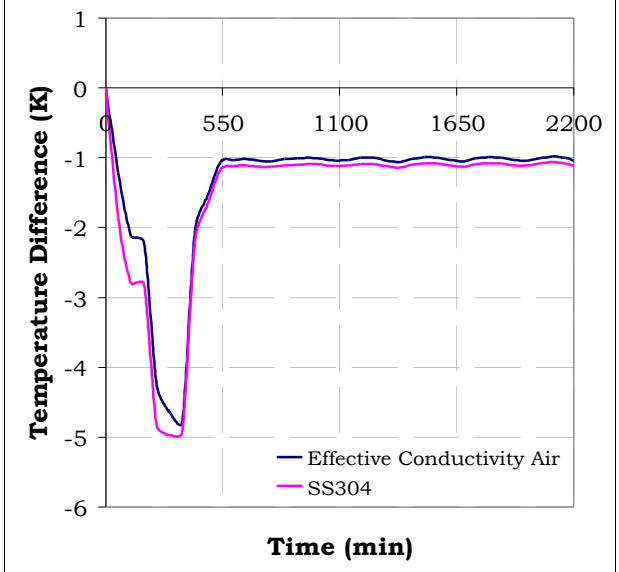

Figure 7. Lid local temperature perturbation due to TC installation

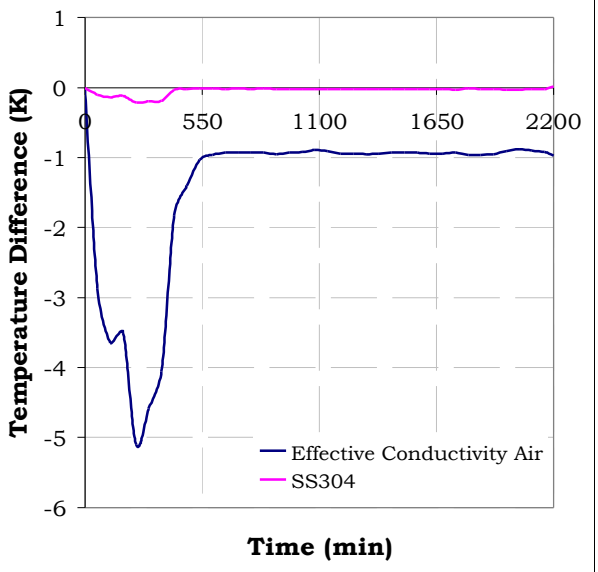

Figure 8. Lid TC temperature indication error (bias) due to installation effects

are documented in Reference 13. A nominal value of 3 W/m^{2}K is used. A fair amount of work[13] was invested in calculating a htc value for the exceedingly-small-diameter TC sheaths. A htc value of 100 W/m^{2}K, which includes radiative and convective heat losses, is used in the simulations.

RADIATION TO ENVIRONMENT

To model thermal radiation to the environment, it was assumed that the environment is a black body at the experimental ambient air temperature. The exposed surface of the can and base (including the partial cavity in the slug) are assigned a nominal emissivity value for stainless steel of 0.3 (Ref. 15). The can exterior sidewalls, base, slug cavity and exposed TC leads are assumed to view the environment with view factors of 1.

COMPARISON OF INITIAL MODEL PREDICTIONS WITH EXPERIMENTAL DATA

Here the initial simulation results are compared against experimental data to assess the accuracy of the boundary conditions applied. Comparisons are first made at the four TCs #5 – 8 on the sidewall of the can (see Figures 1, 2, and 9 for TC locations and IDs). Figure 10 implies that our initial boundary conditions do not provide accurate results at the TC locations along the can wall.

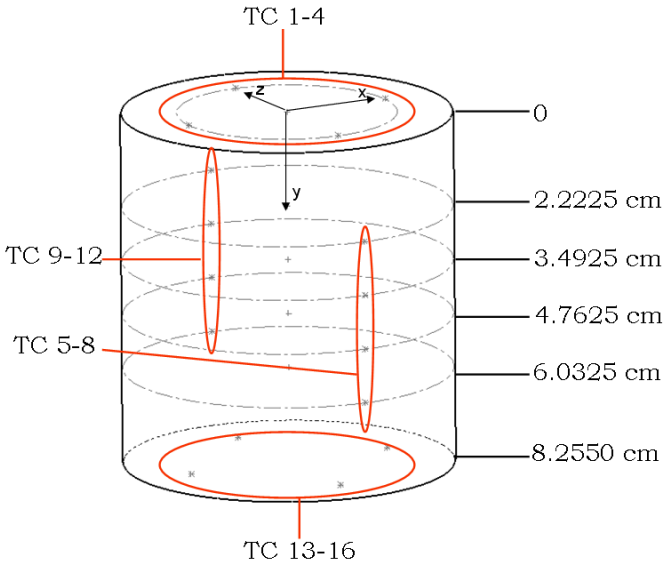

Figure 9. TC locations and IDs

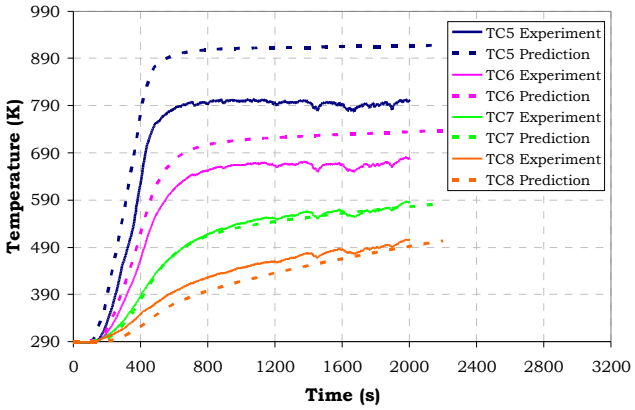

Figure 10. Spatially-uniform heated lid BC predictions compared to measured TC response of can sidewall

The temperature drop from the TC nearest the top of the wall (TC5) to the TC nearest the bottom of the wall (TC8) is approximately 200 K greater with the modeled BCs than for the TC measurements. Sensitivity studies conducted in Reference 13 indicate that a significant portion of this difference can be explained by uncertainty in the particular foam-decomposition thermal model being used, but most of this difference must be rationally attributed to incorrectly modeling the radiative and convective losses from the can walls.

To see whether reasonable uncertainties in the convective and radiative parameters explain the large discrepancies in Figure 10, we reduce the sidewall heat losses by invoking the values at the extremes of the estimated uncertainty ranges (Tamb = 283 K; wall htc = 5.25 W/m^{2}K (50% of nominal); emissivity = 0.15 (50% of nominal)).

Figure 11 reveals that the temperature drop between the highest and lowest sidewall TCs 5 and 8 decreases to about 428 K at 1500 seconds, from a drop of about 437 K at 1500 seconds in Figure 10. Although slight improvement toward the experimental temperature drop of 319 K at 1500 seconds occurs, the results still do not agree well with the measured data. In fact, the overprediction of temperatures at TC5 near the top of the can becomes substantially worse under the lowered radiative and convective cooling of the can walls. Hence, in the following we take a closer look at several initially un-modeled aspects of the experiment.

CORRECTING LID MATERIAL PROPERTIES TO ACCOUNT FOR TC INSTALLATION PLANE

Here we investigate the effect of applying a corrected boundary condition on heated surface of the lid. The lid TCs are located 1 inch radially in from the lid edge, at a depth of ¼ of the lid thickness. The right image in Figure 11 presents the predicted difference between the lid heated top surface and the TC installation plane. This temperature difference is significant, especially at early times. We therefore adjust the lid material properties to effectively thin the lid to ¾ of its thickness so that the computationally convenient application of the temperature BC at the lid surface "acts" like the BC is applied ¼ of the way beneath the surface where the temperature response is actually being measured by the TCs. Since the lid thickness was not changed in the model, the thermal conductivity and density were modified to conserve thermal resistance and heat capacity. Specifically, the thermal conductivity in the direction of the lid thickness is increased by a factor of 1.33 and the density is decreased to 0.75 of its original value, thus eliminating the bias error shown in the image on the right of Figure 11.

RADIAL TEMPERATURE PROFILE OF HEATED LID BC

We note in Figures 10 and 11 that the predicted temperature of TC 5, which is highest on the can sidewall, is respectively about 100K and 170K hotter than the measured temperature. We attribute this in part to the fact that a uniform-temperature BC across the heated plate has been assigned in the model (due to lack of sufficient radial TC placement to determine the lid's radial temperature profile). We reason that the heated lid should be much hotter in the center than at the edges where the lid is welded to the can sidewalls that conduct heat from the lid. Accordingly, the temperature at the edge of the lid should be substantially cooler than that recorded by the four TCs 1-inch in from the edge. Therefore, the imposed uniform-temperature BC on the lid (average of the four TC temperatures) makes the top of the can wall (by virtue of connection to the edge of the lid) considerably hotter than a more realistic radially decreasing temperature profile would. An approximate correction for this is implemented as follows.

Although the radiative power output from the heating lamps was not measured in the experiments, we can approximately solve for this with inverse calculations that adjust the lamp heating level until the predicted lid TC temperature closely matches the measured temperature. The temperature

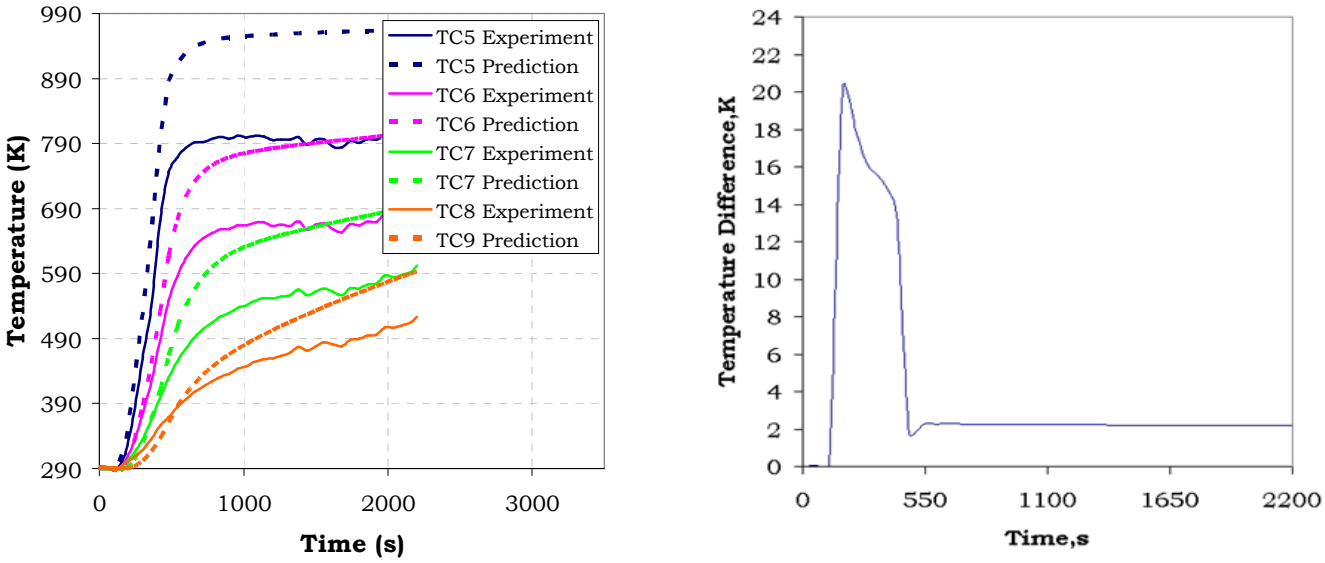

Figure 11. Left: Spatially uniform lid BC with lower-bound radiative/convective modeled sidewall heat losses, compared to measured thermocouple response of can sidewalls. Right: Predicted temperature difference between the top of the FIC lid and the TC installation plane.

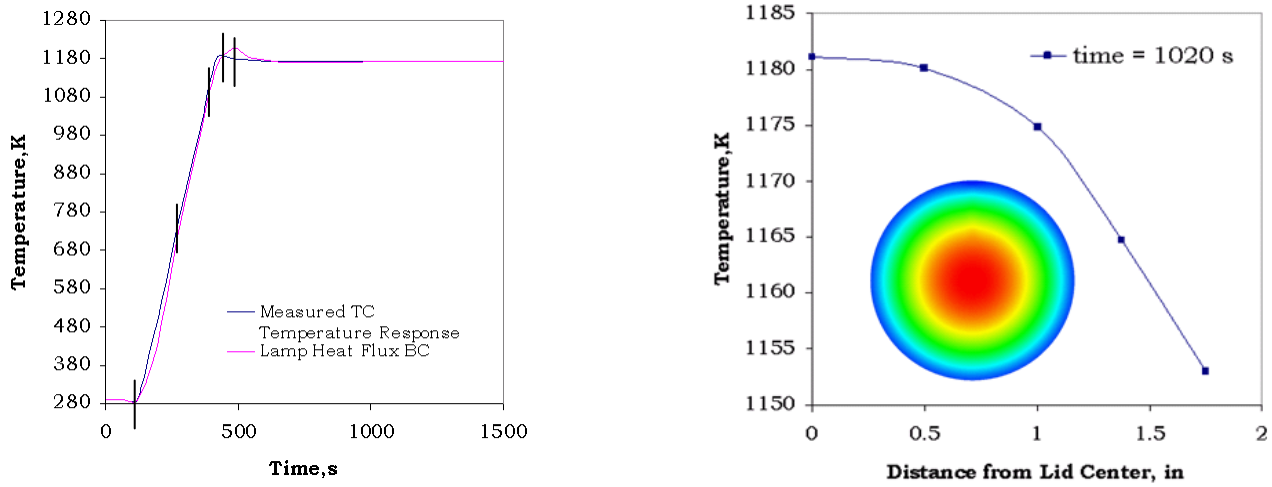

Figure 12. Lamp flux BC lid temperature predictions (Left: measured vs. predicted temperature response at lid TC. Right: predicted radial temperature profile on lid)

profile (shown in Figure 12, left picture) has inflection points as marked at approximate times of 125, 175, 375, 425, and 475 seconds. We also know that incident flux is zero up to about t=125 seconds, and we specify a flux level at 1500 seconds equal to the value at 475 seconds to model the steady temperature condition after approximately 475 seconds. Thus, we have effectively 4 degrees of freedom to solve for, incident flux levels q1, q2, q3, q4 at times of 175, 375, 425, and 475 seconds.

The incident flux on the lid is balanced by radiative and convective heat losses to the environment from the lid top surface, and by heat transferred through the lid to the foam and the can sidewalls (the latter are solved for in the FEM). Local radiative and convective boundary conditions for lid heat loss to the environment depend on the local lid temperature (obtained from the FEM simulation); on the lid emissivity (nominally 0.86 for the Pyromark[14] painted top surface); and on the local htc value that is a weak function of the temperature difference between the ambient air and lid local temperature. The htc value as a function of local temperature is calculated from a relation found in reference 16 and stated in Reference 13. The flux levels q1- q4 include the net incident (after reflection from the lid surface) thermal radiation coming from the lamps and surrounding environment, under the assumption that these sources provide uniform irradiance over the lid.

Initial values of q1- q4 were obtained by using the measured lid temperatures from Figure 12 at the inflection points and calculating the associated radiative and convective heat losses off the top of the lid. An estimated amount of 30% was added to this to account for heat transferred to the foam

and can sidewalls, and the total was used as an initial estimate in an iteration for the incident radiation that would be required to balance these losses. To iterate, after completion of each simulation, adjustment of the flux levels was performed after comparing the predicted lid temperature history at the lid TC location to the actual measured TC response.

Figure 12 shows results of a simulation after 4 iterations to converge on the applied lamp heating flux levels. Again here, lower uncertainty bounds were used for the sidewall convective and radiative losses. The left plot in the figure shows very good agreement between the predicted and target (TC1) temperature responses at TC1's radial location. The right picture in Figure 12 gives an indication of how non-uniform the temperature profile over the lid is. The temperature drop from the center of the lid to the edge is about 27K. The magnitude of temperature drop predicted here is in line with actual measured radial temperature drops in a different test series with another type of foam.[17]

The temperature at the lid edge is about 21 K cooler than at the TC location. Accordingly, the temperature at the top of the can wall is 22 K cooler than if the uniform-temperature BC were being applied. The temperature near TC5 is about 10 K cooler than when the spatially uniform temperature BC is applied across the lid. Thus, the predicted temperatures on the can sidewall move closer to the measured data as shown in Figure 13, but the errors are still large.

ADDING PRESSURE VENT NOZZLES (AS COOLING PIN-FINS) TO THE MODEL

Even with the greater heat losses from the can sidewalls that would accompany more reasonable central values of the estimated convective and radiative conditions, the sensitivity previously shown to these would not in itself be enough to explain the large overprediction in sidewall temperatures (particularly at TC5) shown in Figure 13. In searching for an explanation, we surmise that the pressure fittings shown in Figure 1 act as cooling pin-fins to substantially lower the temperature of TC5 in particular, compared to what it would be if no pressure fitting was in the experiment. Thus, the lack of pressure fittings in the FEM substantially biases the predicted temperature at TC5 upward.

Therefore, the vent nozzles were added to the model as depicted in Figure 14. The vent nozzles are shown to significantly perturb the local temperature field where attached to the can. Figure 15 shows the predicted and measured can sidewall temperatures at TC locations 5 - 8. The much improved agreement at all thermocouples indicates that perhaps the dominant modes of heat transport to and from the can have now been captured in our thermal model of the FIC experiments.

We note that temperature-field type boundary conditions on the can sidewalls (which would ordinarily be expected to be more accurate than trying to model wall convective and radiative fluxes) would be preferable if we had more thermocouple lines at at-least 90 degree intervals between the

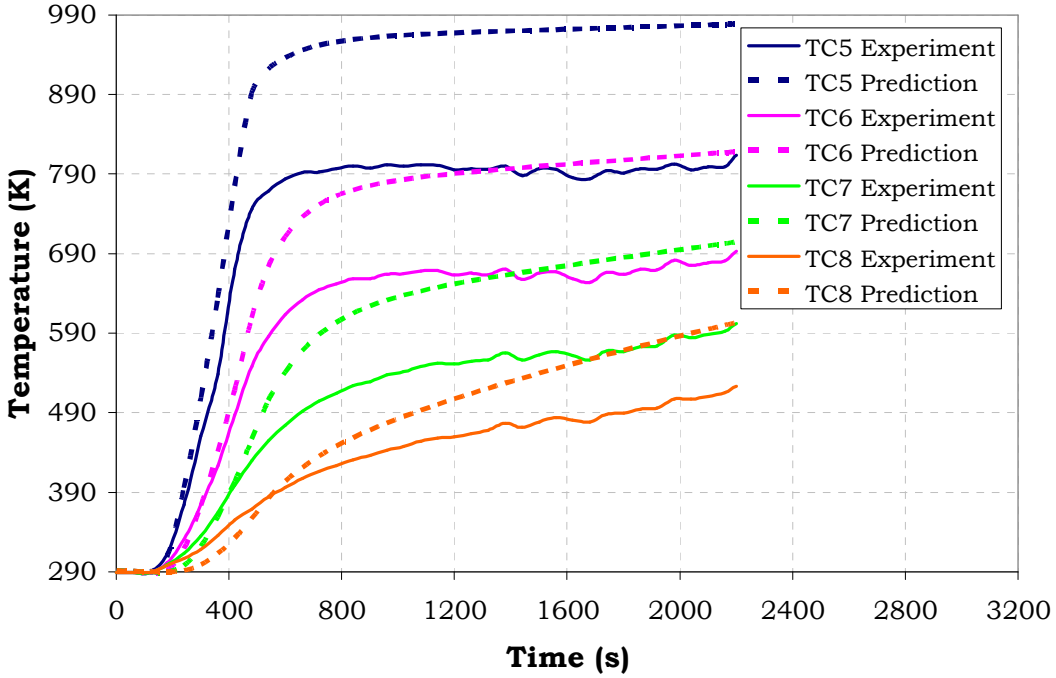

Figure 13. Lamp heat flux heated lid BC predictions compared to measured TC response of can sidewall – with lower-bound radiative/convective sidewall heat losses.

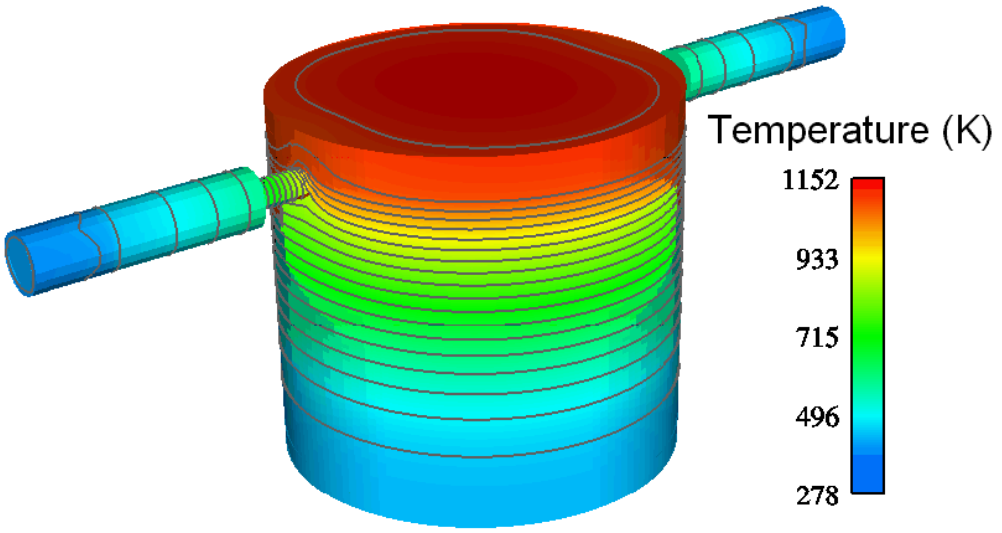

Figure 14. Temperature contours of model predictions with vent nozzles added to model.

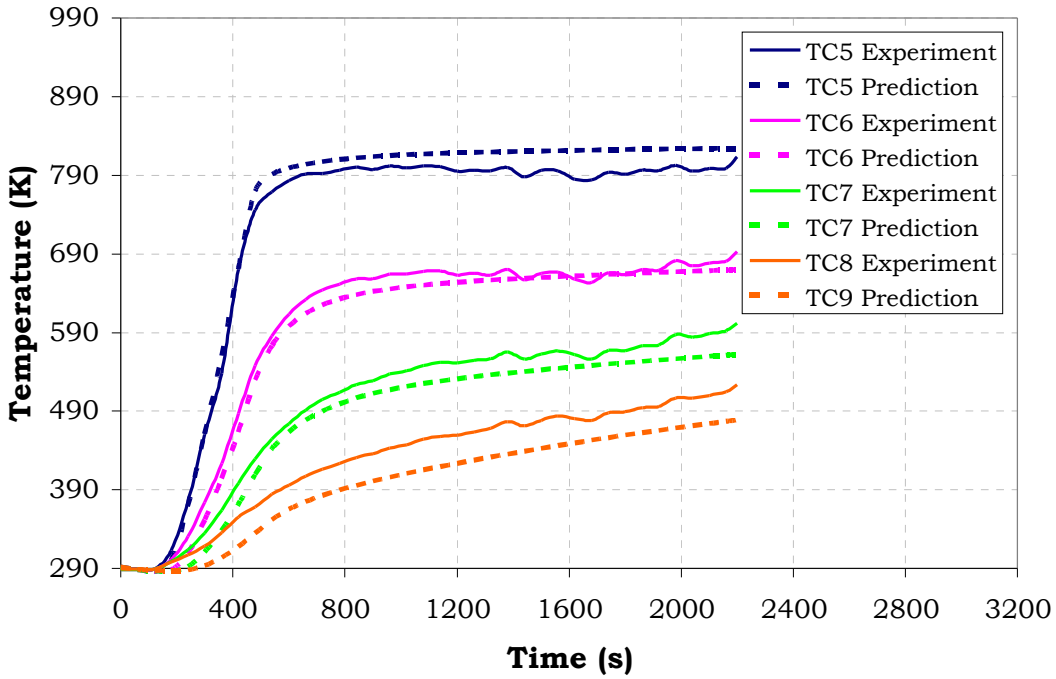

Figure 15. Predictions with vent nozzles added to model, compared to measured TC response of can sidewall – with nominal radiative/convective sidewall heat losses.

existing TC lines. If only two TC lines were possible given the experiment budget, then these lines should be 90 degrees away from their present locations where the nozzles are attached. With the relatively-local temperature perturbation effect from the nozzles as seen in Figure 14, such TC placement would give a more accurate circumferentially-symmetric temperature boundary condition than the present lines of sidewall TCs would.

COMPARISON OF SLUG TEMPERATURE PREDICTIONS TO TC DATA

With the boundary conditions of the experiment now substantially refined in the FEM, the resulting predicted temperature response of the slug TC #18 is shown in Figure 16. The predicted transient response with the final model compares

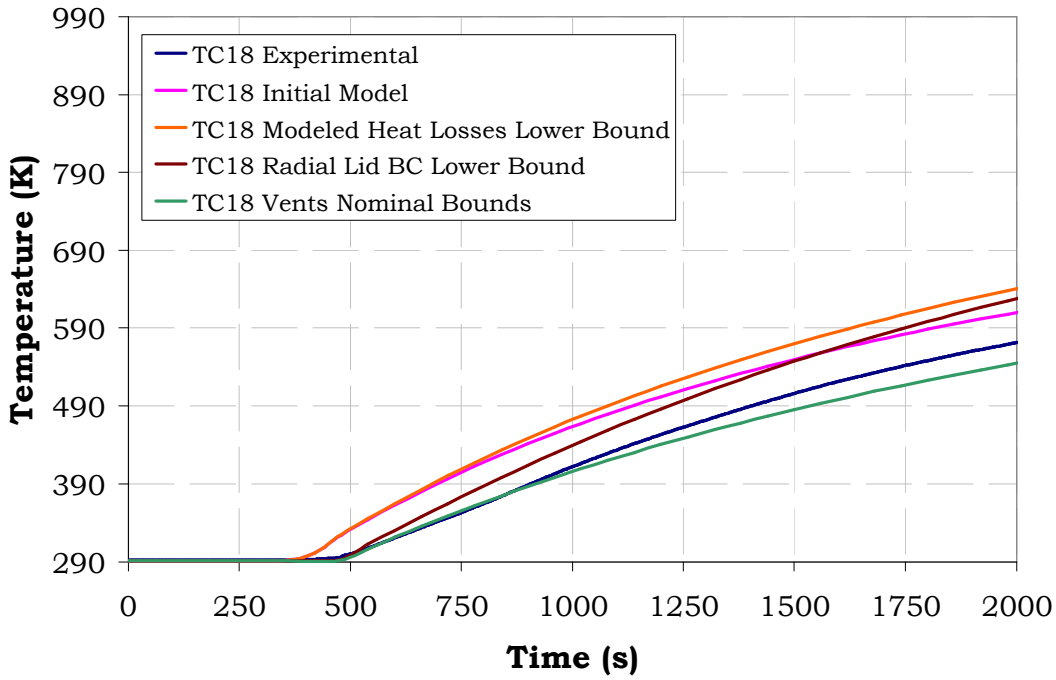

Figure 16. Slug TC18 measured response versus predicted response for various versions of the model.

fairly well with the experimental data. A sensitivity study in Reference 13 shows that reasonable uncertainty of 20% in the foam constitutive submodel's critical porosity parameter affecting its thermal conductivity results in predictions which nicely bound the TC data.

SUMMARY AND CONCLUSIONS

In this paper we have documented some thought processes and the iterative deduction required (propose models; implement models; assess against the experimental data; add or modify models if necessary) to adequately model the boundary conditions and thermocouple response errors in a relatively simple thermal test. We have exposed and explored many difficulties in this process and have shown how these were approximately overcome.

Some of the difficulties resulted from insufficient thermocouple placement on the can lid; from collocation of the vent nozzles with the only lines of thermocouples available for prescribing a temperature-field boundary condition on the can sidewalls (ordinarily expected to be more accurate than trying to model wall convective and radiative losses); and from unmeasured radiative power output from the heating lamps as a function of time. Many of these difficulties arise from unavoidable resource and technology constraints in experiment planning and execution. Nonetheless, the lessons learned here can help minimize avoidable modeling difficulties associated with experiments that feed into model development and validation efforts.

REFERENCES

[1] Erickson, K.L., S.M. Trujillo, J.B. Oelfke, K.R. Thompson, C.R. Hanks, B. Belone, D.M. Ramirez, "Component-Scale Removable Epoxy Foam (REF) Thermal Decomposition Experiments ("MFER" series, April 2003) Supporting the FY04/Q2 Level 1 V&V Milestone. Part 1: Temperature Data," Sandia National Laboratories report in revision.

[2] Attia, M.H., Cameron, A. and Kops, L. Distortion in Thermal Field Around Thermocouples in Experimental Interfacial Studies, Part 4: End Effects. *Journal of Manufacturing Science and Engineering*, 124:135, February 2002

[3] Satyamurthy, P., R.K. Marwah, N. Venkatramani, V.K. Rohatgi, "Estimation of Error in Steady-State Temperature Measurements Due to Conduction along the Thermocouple Leads," *Intn'l. J. Heat and Mass Transfer*, Vol. 22,

[4] Romero, V.J., M.P. Sherman, J.D. Johnson, J.F. Dempsey, L.R. Edwards, K.C. Chen, R.V. Baron, C.F. King, "Development and Validation of a Component Failure Model," paper AIAA2005-2141, 46th AIAA/ASME/ASCE/AHS/ASC Structures, Structural Dynamics, and Materials Conference, April 18-21, 2005, Austin, TX.

[5] J.A. Nakos, "Understanding the Systematic Error of a Mineral Insulated, Metal Sheathed Thermocouple Attached to a Heated Flat Surface. L.A. Gritzo and N. Alvarez, editors, Thermal

Measurements: The Foundation of Fire Standards, number STP 1427, ASTM 2002.

[6] J.A. Nakos, "Understanding the Systematic Error of a Mineral Insulated, Metal Sheathed Thermocouple Attached to a Heated Flat Surface. L.A. Gritzo and N. Alvarez, editors, Thermal Measurements: The Foundation of Fire Standards, number STP 1427, page 32. ASTM 2002.

[7] Figueroa, V., "Effects of Parameter Variations Associated with 1/16" Mineral Insulated Metal Sheathed Thermocouples Installation on the Surface Temperature Measurement of a Uniformly Heated Plate," University of New Mexico School of Mechanical Engineering M.S. Thesis report, April 27, 2006.

[8] *Manual on the Use of Thermocouples in Temperature Measurements*. No. 12. ASTM Publication, 4th Edition, 1993.

[9] Nakos, J.A., "Uncertainty Analysis of Thermocouple Measurements Used in Normal and Abnormal Thermal Environment Experiments at Sandia's Radiant Heat Facility and Lurance Canyon Burn Site," Sandia National Laboratories report SAND2004-1023 printed April 2004.

[10] Shelton, J.W., V.J. Romero, D. Dobranich, M.P. Sherman, Sandia National Laboratories SAND report in preparation.

[11] Karlekar, V., and R.M. Desmond, *Engineering Heat Transfer*, West Publishing Co, 1977.

[12] Incropera and Dewitt, *Fundamentals of Heat and Mass Transfer, 4th Edition*, 1996

[13] Shelton, J.W., V.J. Romero, D. Dobranich, M.P. Sherman, Sandia National Laboratories SAND report in preparation.

[14] http://calore.sandia.gov/index.php

[15] Incropera and Dewitt, *Fundamentals of Heat and Mass Transfer, 4th Edition*, 1996

[16] Karlekar, V., and R.M. Desmond, *Engineering Heat Transfer*, West Publishing Co, 1977.

[17] Chu, T.Y., M.L. Hobbs, K.L. Erickson, T.A. Ulibarri, A.M. Renlund, W. Gill, L.L. Humphries, T.T. Borek, "Fire-induced Response in Foam Encapsulants," in Proceedings SAMPE 1999-44th Intn'l. SAMPE Symposium & Exhibition (1999).